THE AMERICAN MINERALOGIST, VOL. 56, MAY–JUNE, 1971

COMPOSITIONAL SECTOR-ZONING IN CLINOPYROXENE FROM THE NARCE AREA, ITALY

LINCOLN S. HOLLISTER AND ALEXANDER J. GANCARZ,
Department of Geological and Geophysical Sciences
Princeton University, Princeton, N. J. 08540

ABSTRACT

An electron microprobe study of sector-zoning in clinopyroxenes from the Narce area, Italy shows that the relative order of enrichment of the pyroxene components with trivalent or quadrivalent cations in the *M*1 sites in the four crystallographically distinct sectors, (100), (110), (010), ($\bar{1}$11), is (100)>(110)>(010)>($\bar{1}$11). For the crystal showing the largest amount of sector-zoning, the (100) sector has about 5% more $CaAl_2SiO_6$, 4% more $CaFe^{3+}AlSiO_6$, 1% more $NaTiAlSiO_6$, and 1% more $CaTiAl_2O_6$ than the ($\bar{1}$11) sector.

In order to interpret the sector-zoning in clinopyroxene, the model developed to interpret sector-zoning in staurolite (Hollister, 1970) is expanded to include effects of the atomic configurations on the surfaces of growth steps and the properties of the material added to a growing crystal. It is concluded that there are at least four controlling factors involved in developing compositional sector-zoning: size and composition of ionic complexes added to the crystal as it grows, rate of addition of material, rate of equilibration of the new material with the matrix at the surfaces of growth steps, and rate of re-equilibration of surface layers with the matrix by exchange of ions perpendicular to the crystal faces.

The fact that pyroxene from a lava flow can be sector-zoned in the component $CaAl_2SiO_6$ suggests that care should be exercised in interpreting the presence of this component in a crystal as indicative of crystallization in a high pressure environment, especially in the absence of co-crystallization of anorthite.

INTRODUCTION

A crystal which is compositionally sector-zoned (Hollister, 1970) has different regions, or sectors, which have significant differences in composition. These chemical differences are probably produced on the surfaces of simultaneously growing crystal faces, under identical conditions of pressure, temperature and composition. A euhedral crystal can be thought of as made of a set of pyramids with the crystal faces as bases of the pyramids and the apices of the pyramids coincident at the crystal center (Fig. 1). All pyramids that have for their bases faces of the same crystal form are collectively named by the face characterising that form. Referring to Figure 1, a sketch of a clinopyroxene crystal with the forms {100}, {010}, {110}, and {$\bar{1}$11}, there are four distinct sets of pyramids that are designated the (100), (010), (110), and ($\bar{1}$11) sectors. One pyramid of the (010) sector (there are two such pyramids) is shown schematically in the sketch.

It was shown by Hollister (1970) that for the mineral staurolite the compositions of each sector can be markedly different. The data were interpreted to be the result of initial surface equilibrium which was

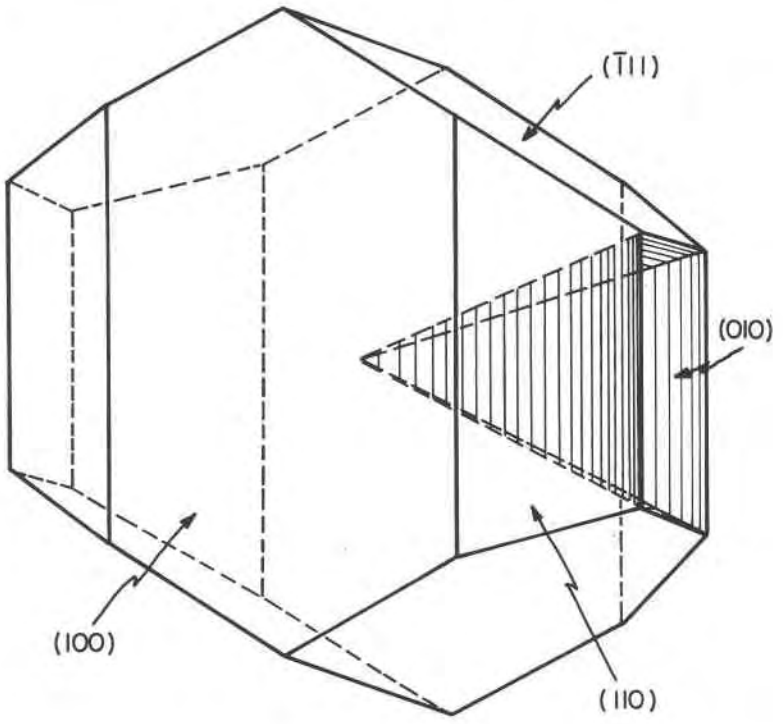

FIG. 1. Sketch of clinopyroxene crystal with forms {100}, {010}, {110}, and {111}. Volume of (010) sector shown schematically.

achieved by chemical exchange between the matrix and the distinctly different two-dimensional atomic arrangements on each face. The compositions on the faces are preserved if the rate of growth of the crystal exceeds the rate of exchange between the interior of the crystal, with a three-dimensional atomic configuration which is identical in each sector, and the matrix. Thus, the presence of compositional sector-zoning in a mineral is apparently indicative of rapid growth of that mineral. In support of this hypothesis, perhaps the best examples of compositional sector-zoning are in some of the lunar clinopyroxenes from the Apollo 11 landing site (Hargraves, *et al.*, 1970; Hollister and Hargraves, 1970; Albee and Chodos, 1970) which are generally considered to have grown in a melt which crystallized rapidly.

On the other hand, most petrologists attempt to infer the pressure and temperature conditions of formation of a rock from the composition of a particular mineral (see Binns, *et al.*, 1970, for a recent example pertaining to clinopyroxene) or to the partition of elements between coexisting

minerals. Because sector-zoning can result in major differences of chemistry between different volumes, or sectors, which have grown under identical conditions of pressure, temperature, and composition, it is important to know what factors control sector-zoning and in what components a mineral may be sector-zoned. That is, those factors which cause differences in the concentration of a component between adjacent sectors of a mineral will thereby affect the bulk composition of the whole crystal as well as the bulk composition of a sector.

The present study presents a description of compositional sector-zoning in clinopyroxenes from the Narce area, 40 km north of Rome, Italy. The observations point to complexities additional to those in the idealized model presented for the mechanism of sector-zoning in staurolite (Hollister, 1970) but suggest that as a result of these additional complexities more insight can be obtained on the mechanisms by which crystals grow as well as to the relative rates of growth of crystals. Furthermore, the data show that a pyroxene crystal can be sector-zoned in the component $CaAl_2SiO_6$. The presence of this component in clinopyroxenes coexisting with anorthite and in the absence of garnet is generally thought to reflect pressure of crystallization (Kushiro, 1962, 1965; Clark, *et al.*, 1962; Kuno, 1964). The data in the present paper suggest that in addition to a possible pressure dependence on the overall amount of $CaAl_2SiO_6$ in pyroxene, the absolute amount may depend in part on the rate of growth of the pyroxene.

Strong (1969) has summarized much of the early work on hourglass structures in pyroxene. Bence, *et al.* (1970a) describe sector-zoning in clinopyroxene from Terlingua, Texas, which is similar to that described in the present paper. References to descriptions of compositional sector-zoning in other minerals are given in Hollister (1970), and Poty (1966).

Sample Description

Samples were collected from a Pliocene-Pleistocene volcanic terrane in the Narce area, which is within the alkali magmatic province of western central Italy. In general, the volcanic rocks are trachytic in composition, but the investigated specimens are interpreted by Marinelli and Mittempergher (1966) to be late stage magmatic products which show signs of extreme differentiation towards potassium-rich rocks. The typical late stage magmatic product is a leucite phonolite.

The leucite phonolite lavas are intercalated with a stratified tuff. These rock types compose the stratigraphically highest unit in the Narce area. The columnar jointed laval flows occur as discrete lenticular units which, in cross section, are 200–300 meters wide and 10–15 meters thick. At the base of each flow is a 1–2 meter thick zone of volcanic breccia.

The Narce area was first comprehensively mapped by Mattias (1969). Previous work by Washington and Merwin (1921) at Mt. Vesuvius, also within the alkali magmatic province, revealed euhedral phenocysts of clinopyroxene with a crystal morphology similar to that of the studied specimens (*i.e.*, forms $\{100\}$, $\{010\}$, $\{110\}$ and $\{\bar{1}11\}$, Fig. 1).

In addition to the phenocrysts of clinopyroxene, there are phenocrysts of leucite and

sanidine set in a very fine-grained matrix composed of pyroxene, leucite, sanidine, and magnetite. The pyroxene phenocrysts have a mean grain dimension of 0.5 mm and show conspicuous sectoral differences not only in color, but also in the angle of extinction (Fig. 2). Additional description of the samples and their geologic setting may be found in Gancarz (1970).

Analytical Procedure

A universal stage was used to unambiguously identify the growth forms of the pyroxene phenocrysts. Of the 18 crystal sections examined, seven favorably oriented ones were selected for electron microprobe analyses. Analyses were made for three elements simultaneously with an ARL-EMX-SM microprobe at 2 to 6 micron intervals across each crystal. Operating conditions were 15 kilovolts and about .05 microamperes sample current. Beam diameter was less than 1 μm except for the Na analyses, for which a beam diameter of 20 μm, at 15 kilovolts and .05 microamperes, was required to avoid volatilization of Na. Three traverses, in different crystallographic directions, were made across most of the crystal sections. Most traverses were at the shorter step interval of 2 microns. Each traverse was repeated three times in order to obtain element profiles of all major elements in abundance greater than 0.01 weight percent as the oxide: Na, Mg, Al, Si, Ca, K, Ti, Mn, and Fe. The data of two crystal sections from one rock, which had both directions of prismatic (110) cleavage vertical and which had differences in the size of the section across the ($\bar{1}$11) sectors (Fig. 2), are discussed in this paper. The other data generally support the conclusions but are not presented because they came from different rocks and therefore are not directly correlatable to the data presented.

The counting rates for each element at points on either side of sector boundaries were determined visually from the zoning profiles. This reduced precision at each point, but it is extremely difficult to locate, in the microprobe, points only a few microns apart on either side of a sector boundary. Because of both continuous and discontinuous in-sector zoning (Fig. 3), points could not be separately analyzed in each sector and averaged to obtain meaningful results. The method used, however, gives more accurate and meaningful results than one requiring relocation of the analysis site.

The counting rates for each analysis point were corrected for deadtime and background and divided by the deadtime and background corrected counting rates of appropriate standards. The weight percent of each oxide was obtained from these ratios by the correction procedure of Bence and Albee (1968) as modified by Albee and Ray (1970). It is important to here emphasize that all the major conclusions of this paper are dependent on differences in concentration across sector boundaries and therefore are *not* substantially dependent on instrumental drift between time of analysis on sample and standard or on systematic errors introduced by the correction procedure, analytical procedure, or in errors in the analyses of the standards.

For 56 total analyses determined in the above manner, the summation of 30 was between 98.5 and 99.5 percent, assuming all iron as divalent and all titanium as quadrivalent. All but four of the remainder totaled less than 98.5 percent. An almandine garnet used as an internal standard had an oxide sum of 100.3% with 3.00 Si atoms and 1.98 Al atoms to a formula unit based on 12 oxygen atoms. This test indicates a reasonable accuracy for the pyroxene analyses and indicates that the low totals are probably in part the result of extra oxygen associated with trivalent iron.

Results

Figures 3a and 3b are zoning profiles for seven elements across sections cut nearly perpendicularly to the *c*-axes of two different crystals from one

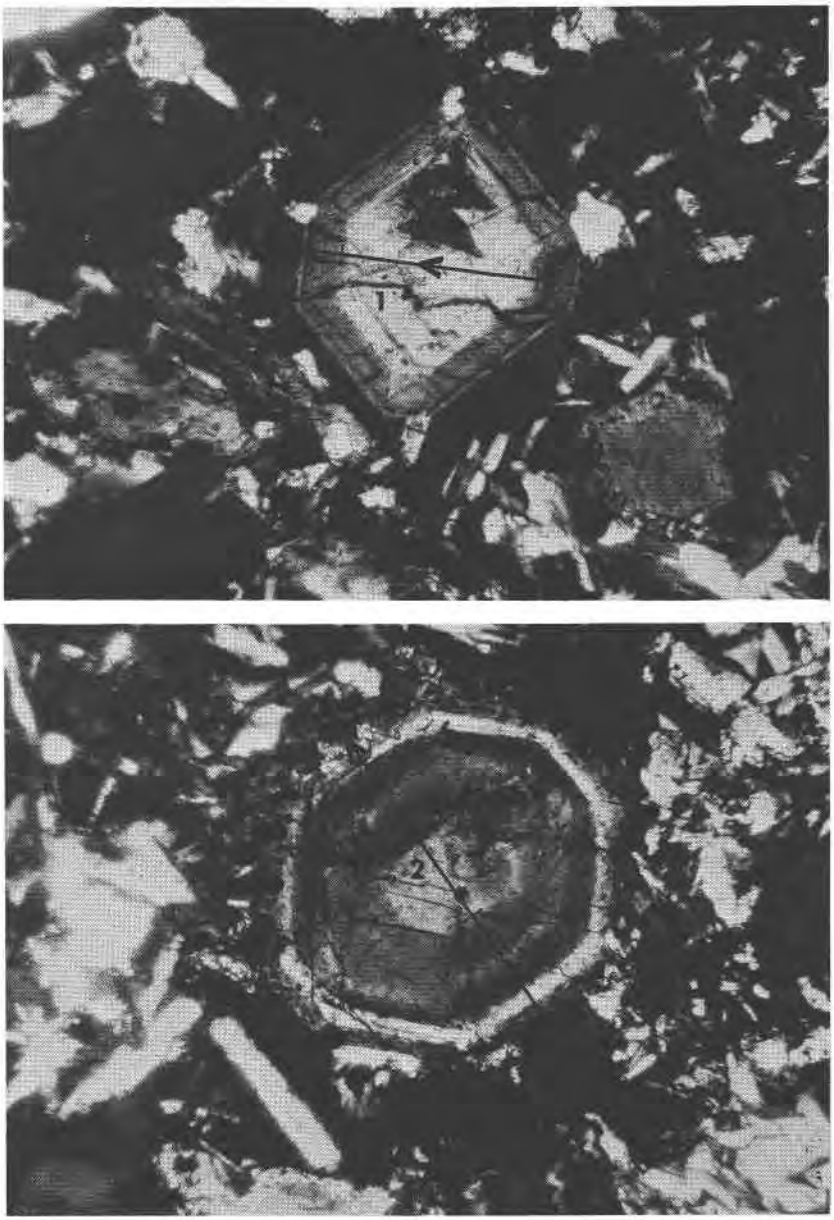

FIG. 2. Photomicrographs (crossed polarizers) of sections through crystal 1 (Figure 2a) and crystal 2 (Figure 2b). Both sections are nearly normal to the z direction, and the prismatic cleavage, parallel to {110}, is clearly visible. Each marked traverse begins and ends on a face of the {100} form. The positions where the traverses cross sector boundaries are marked. Traverse 1 is 0.3 mm long; traverse 2 is 0.33 mm long.

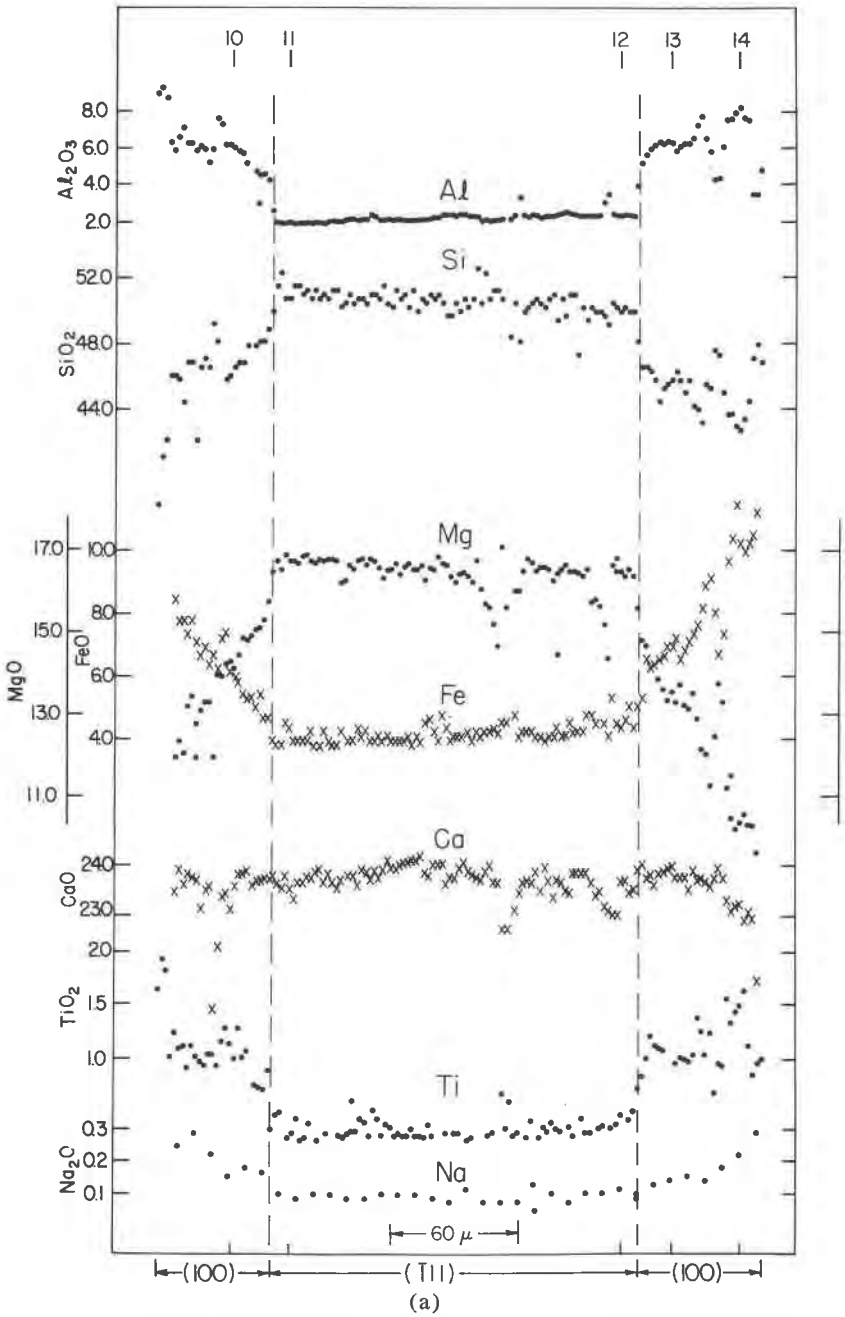

(a)

FIG. 3. Variations of the elements Al, Si, Fe, Mg, Ca, Ti, and Na along traverses 1 and 2 and (T11) sectors. Oxide scales are based on analyses determined at points

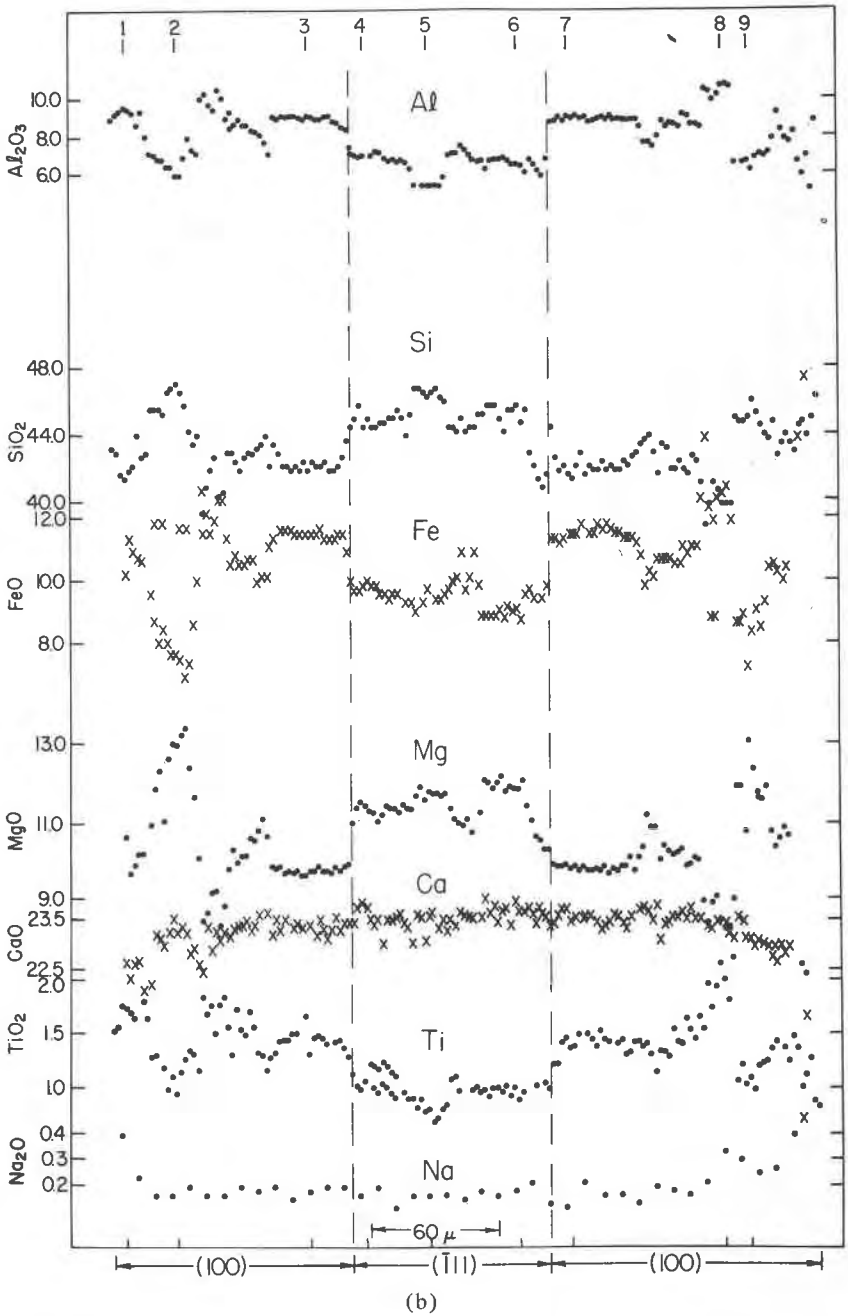

(b)

of crystals 1 and 2 (Figure 2). Vertical dashed lines mark boundaries between the (100)
1–14. Electron-beam diameter is less than 1 μm; analysis interval is 2 μm.

rock. Each profile begins at a crystal edge, passes through the (100) sector into the ($\bar{1}11$) sector, back into the (100) sector, and ends at the crystal edge opposite the starting point. The sector boundaries are indicated by vertical dashed lines. Both crystals contain small amounts of K and Mn as well as the elements illustrated (Table 1), and the scales for both profiles were determined by analyses at the points 1–14 by the method outlined in the previous section.

The crystals are clearly sector-zoned in all elements (Fig. 3 and Table 1); however, the magnitude of the differences in composition is greater for the crystal of Figure 3a, which was cut relatively further from the crystal center than the crystal of Figure 3b, as indicated by the wider section through the ($\bar{1}11$) sectors. The difference in magnitude of sector-zoning is mainly due to the difference in composition between the ($\bar{1}11$) sectors of the two crystals. A longitudinal profile from center to edge entirely within the ($\bar{1}11$) sector of another crystal showed at the center a

TABLE 1. ANALYSES OF CLINOPYROXENE SECTORS

	Crystal 1				*Crystal 2*			
Sector	(100)	($\bar{1}11$)	(010)	(110)	(100)	($\bar{1}11$)	(010)	(110)
SiO_2	46.40	50.25	46.86	45.70	42.35	44.79	44.00	44.45
TiO_2	1.32	0.75	0.86	1.00	1.48	1.08	1.35	1.37
Al_2O_3	6.43	2.42	5.23	5.86	9.20	7.06	8.32	8.09
FeO[a]	6.48	4.78	6.34	6.38	11.53	9.90	11.12	10.73
MnO	0.06	0.09	0.09	0.12	0.17	0.09	0.08	0.10
MgO	14.07	16.59	13.91	13.46	9.85	11.33	10.62	10.52
CaO	23.83	23.73	23.70	23.57	23.36	23.58	23.52	23.49
Na_2O	0.23	0.10	0.21	0.21	0.19	0.19	0.18	0.19
K_2O	0.02	0.01	0.01	0.01	0.01	0.01	0.01	0.01
Total	98.85	98.71	97.20	96.31	98.13	98.03	99.18	98.18
	Atoms on the basis of 6 oxygen atoms							
Si	1.758	1.881	1.802	1.778	1.662	1.740	1.700	1.716
Al	.242	.107	.198	.222	.338	.260	.300	.284
Al	.045	.000	.039	.047	.088	.067	.079	.085
Mg	.794	.926	.797	.781	.576	.656	.612	.606
Ti	.038	.021	.025	.029	.044	.032	.039	.040
Fe	.205	.150	.204	.208	.378	.322	.359	.347
Ca	.967	.952	.977	.983	.982	.982	.974	.972
Mn	.002	.003	.003	.004	.006	.003	.002	.003
Na	.017	.008	.015	.016	.014	.015	.013	.014
K	.001	.000	.001	.000	.000	.000	.000	.000

[a] All Fe calculated as FeO

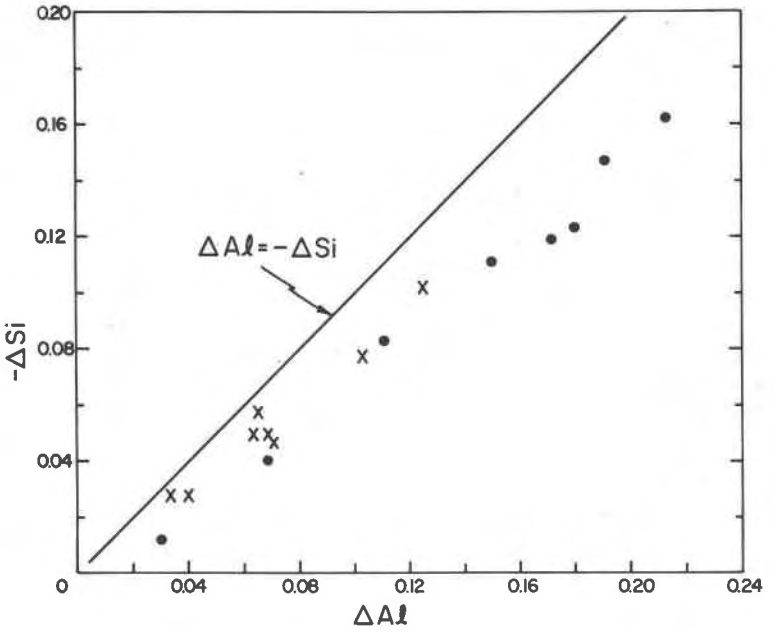

FIG. 4. Plot of differences in atomic proportion of Al against difference in atomic proportion of Si across sector boundaries. Crystal 1 (●) Crystal 2 (×).

composition similar to that of the ($\bar{1}11$) sector of Figure 3b. A composition similar to that of the ($\bar{1}11$) sector of Figure 3a was attained after a series of jumps in composition within the ($\bar{1}11$) sector along the longitudinal profile towards a face of the {$\bar{1}11$} crystal form. Thus, it appears that over most of the growth of the clinopyroxene crystals the differences in composition across sector boundaries increase with growth. This point is qualitatively illustrated in Figures 4 and 5.

Figure 4 shows the difference in composition in Al and Si atoms across the boundaries between the (100) and ($\bar{1}11$), (010) and ($\bar{1}11$), (110) and ($\bar{1}11$), and (100) and (110) sectors of each of the two crystals shown in Figure 2. The data used for the plot are listed in Table 2. The 45° line shows where the points should fall if Al substituted for Si only. Since Al substitution for Si can be balanced by substitution of Al, Fe^{3+} or Ti^{4+} for divalent cations, the excess change in Al (Fig. 4) implies that Al, in addition to Fe^{3+} and Ti^{4+}, substitutes for divalent cations.

The data as plotted in Figure 5 confirm the above conclusion. They show that the change in excess Al atoms is essentially balanced by a change in the sum of Ca, Fe, and Mg atoms.

The sector-zoning in $CaFe^{3+}AlSiO_6$ appears to be due to a relative enrichment in the $M1$ sites of the (110), (010), and (100) sectors in atoms

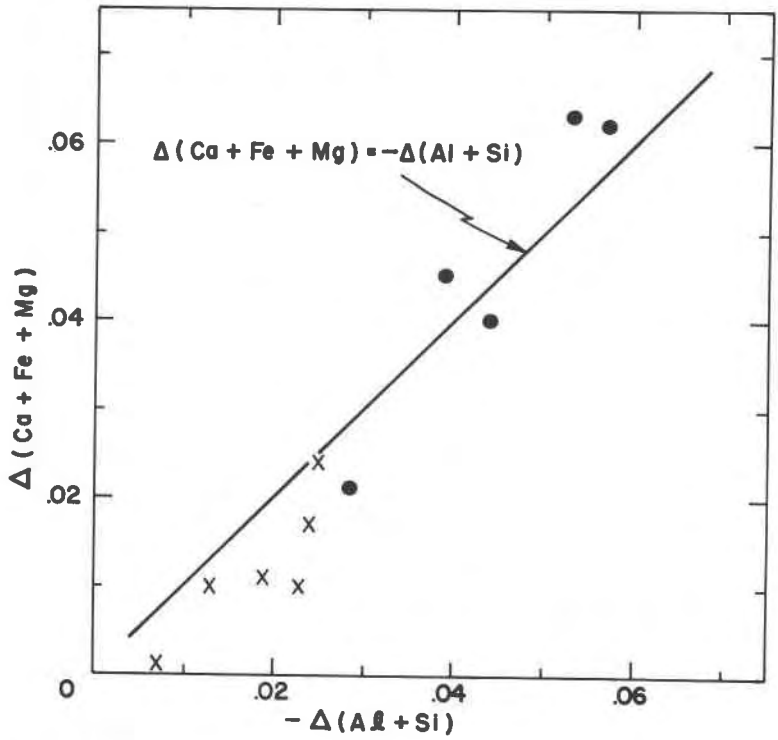

FIG. 5. Plot of difference in the atomic sum (Ca+Fe+Mg) against difference in atomic sum (Al+Si) across sector boundaries. A point on the line implies Al substitution for (Ca+Fe+Mg). Crystal 1 (●); Crystal 2 (×).

of Fe^{3+} rather than in oxidation of Fe^{2+} atoms already present in those sectors. This conclusion is based on the data plotted in Figure 6. The scale along the vertical axis is the difference between sectors in the sum of Al, Mg, Si, and Ti atoms and can be shown to be equivalent to a calculated difference of the atomic sum ($Fe^{2+}+Fe^{3+}$) in the *M*1 sites. The scale along the horizontal axis is the difference between sectors in the sum of 2 Si, 2 Ti ,and Al and can be shown to be equivalent to the change in sectors of Al in the tetrahedral sites as a result of a change in Fe^{3+}, either atomic or as oxidized Fe^{2+}, in the *M*1 sites. A point falling on the 45° line would imply that the change of ($Fe^{2+}+Fe^{3+}$) in the *M*1 site is equal to the change in amount of Fe^{3+}. If this were the case, the charge change between sectors due to Al substitution for Si, corrected for Ti and Al in the *M*1 sites, would be due to sector-zoning in atoms of Fe^{3+}. That is, the sector-zoning in $CaFe^{3+}AlSiO_6$ would not be due to Fe^{2+} being oxidized to Fe^{3+} but rather Fe^{3+} substituting for Mg, Ti, and Al. A point

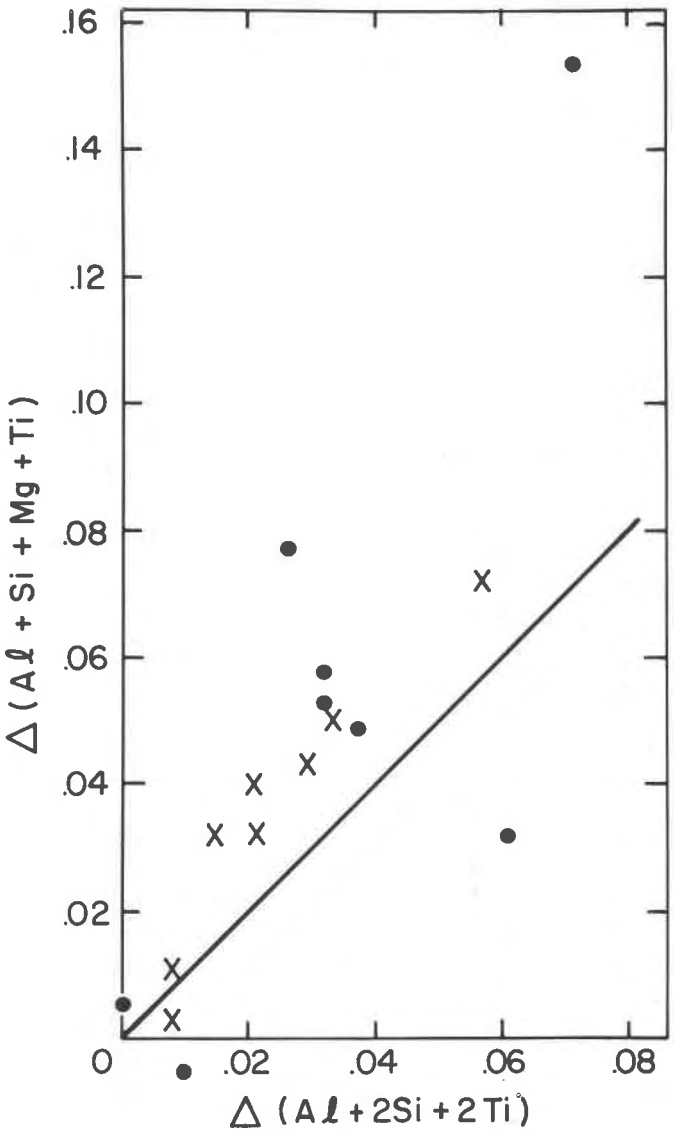

FIG. 6. Plot of difference in the atomic sum (Al+Mg+Si+Ti) against difference in atomic sum (2Si+2Ti+Al) across sector boundaries. Crystal 1 (●); Crystal 2 (×). See text.

below the line would imply oxidation of Fe^{2+} to Fe^{3+} and a point above the line would imply that both Fe^{3+} and Fe^{2+} substitute for Mg, Ti, and Al in the sectors enriched in $CaFe^{3+}AlSiO_6$. The fact that most of the

TABLE 2. DATA USED FOR FIGURES 4–7
Atoms on the basis of 6 oxygen atoms

Sector	Ca	Na	K	Mn	Mg	Ti	Fe	Al	Si
				Crystal 1					
(100)	.967	.017	.001	.002	.794	.038	.205	.287	1.578
($\bar{1}$11)	.952	.008	.000	.003	.926	.021	.150	.107	1.881
(100)	.964	.017	.001	.002	.835	.037	.170	.280	1.762
($\bar{1}$11)	.955	.008	.000	.002	.932	.016	.122	.089	1.909
(110)	.982	.016	.000	.004	.779	.034	.219	.275	1.764
($\bar{1}$11)	.971	.010	.001	.003	.891	.014	.163	.125	1.875
(110)	.983	.016	.000	.004	.781	.029	.208	.269	1.778
($\bar{1}$11)	.970	.007	.000	.003	.931	.009	.134	.097	1.897
(010)	.977	.015	.001	.003	.797	.025	.204	.237	1.802
($\bar{1}$11)	.964	.014	.000	.003	.883	.016	.152	.126	1.885
				Crystal 2					
(100)	.989	.014	0	.006	.584	.041	.377	.428	1.656
($\bar{1}$11)	.981	.014	0	.003	.690	.030	.289	.303	1.758
(100)	.982	.014	0	.006	.576	.044	.378	.426	1.662
($\bar{1}$11)	.982	.015	0	.003	.656	.032	.322	.323	1.740
(110)	.971	.014	0	.003	.598	.042	.357	.383	1.701
($\bar{1}$11)	.971	.014	0	.003	.664	.003	.292	.318	1.759
(110)	.972	.014	0	.003	.606	.040	.347	.369	1.716
($\bar{1}$11)	.973	.014	0	.003	.667	.032	.297	.306	1.766
(010)	.968	.013	0	.002	.610	.035	.359	.372	1.713
($\bar{1}$11)	.974	.014	0	.003	.670	.031	.310	.301	1.760
(010)	.974	.013	0	.002	.612	.039	.359	.379	1.700
($\bar{1}$11)	.975	.014	0	.003	.668	.034	.313	.310	1.750

data points define a trend above the line suggests that Fe^{3+} and Fe^{2+} are both enriched in the *M*1 sites of the (110), (010), and (100) sectors relative to the ($\bar{1}$11) sector.

The relative enrichment of Ti in sectors may not be the same for all clinopyroxenes (Bence, *et al.*, 1970a; Albee and Chodos, 1970; Hollister and Hargraves, 1970). The order of Ti enrichment suggested by Hollister and Hargraves (1970) for the Apollo 11 lunar clinopyroxenes is (010) > (001?) > (110). Bence, *et al.* (1970a) argue that this identification is incorrect because they find the following order of Ti enrichment in pyroxenes from Terlingua, Texas: (110) = (100) > (010) > (001) or (011).[1] Albee and Chodos (1970) essentially agree with Hollister and Hargraves (1970) that the (010) sector of the lunar clinopyroxenes from the coarser-grained rocks appears to be the most enriched in Ti.

[1] The (011) and ($\bar{1}$11) sectors are the same; notation depends on choice of positive direction of *a*-axis.

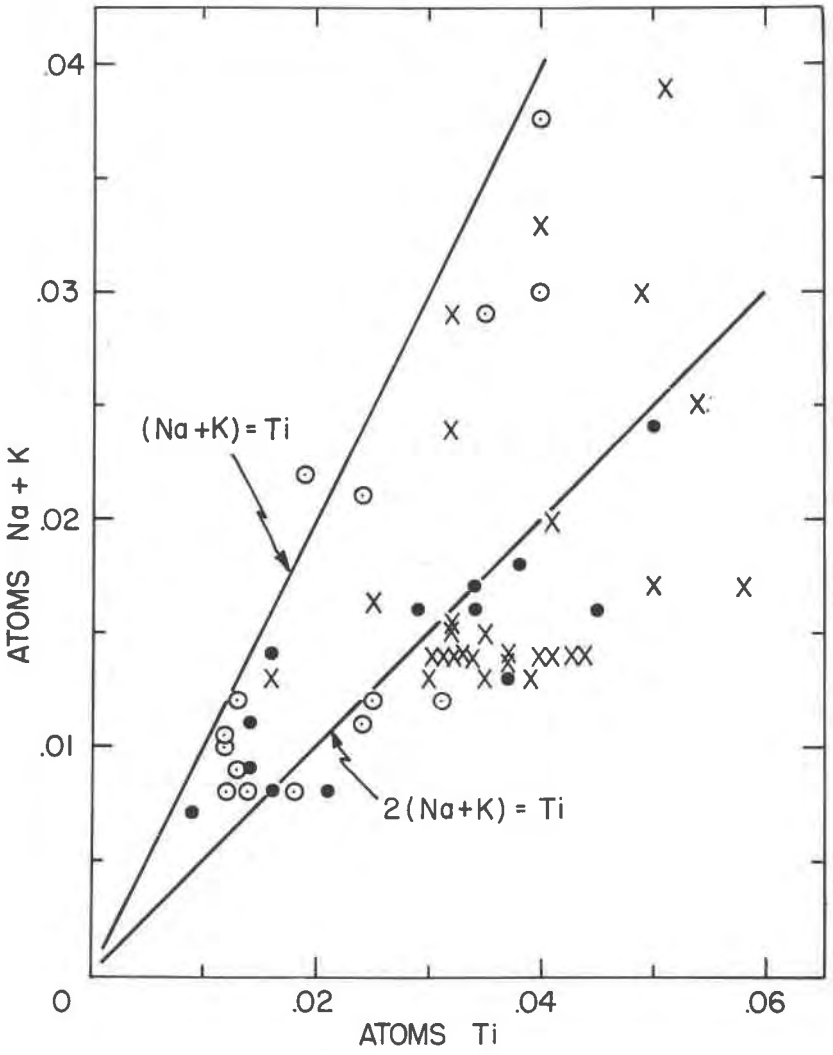

FIG. 7. Plot of the atomic sum (Na+K) against Ti for individual analyses from crystal 1 (●), crystal 2 (×), and other crystals from the Narce area (⊙). See Text.

The data shown in Table 2 and Figure 7 are essentially in agreement with those of Bence, *et al.* (1970a) for the Terlingua samples. The relative enrichment of Ti between sectors of one crystal (table 3) is (100) > (110) > (010) > ($\bar{1}$11), and the relative enrichment between sectors of the other crystal as (100) ≈ (110) > (010) > ($\bar{1}$11). However, the (001) sector is not present in the Narce area samples; and it is not clear that the (100)

sector is present in all the clinopyroxenes from all the coarser-grained Apollo 11 lunar samples. The fact that Ti appears to be involved in two different coupled substitutions (see below) further complicates the matter. The implication of the order of Ti enrichment in sectors of pyroxenes, as well as Al and Fe^{3+} in $M1$, to the model of sector-zoning for staurolite proposed by Hollister (1970) is discussed in the next section.

The data of Figure 7 suggest that Na follows Ti in the pyroxene structure. There is also a small sectoral difference in (Na+K) in crystal 1 (Table 2) which has the same relative order of enrichment as Ti. These data suggest (Na+K) is involved with Ti in a coupled substitution, possibly Na+Ti=Ca+Al. The basis for the proposal of this couple is the assumption that Na substitutes for Ca and that atomic and charge balance must be maintained in any coupled substitution. If there is a significant trend in the data of Figure 7, it is about the line 2(Na+K) =Ti. This would imply that the proposed couple Na+Ti=Ca+Al accounts for about half the Ti in the pyroxene, and that it is partly involved in the sector-zoning of Ti along with the well-known couple Ti+2Al=R^{2+}+2Si. The difference in magnitude of sector-zoning of Ti between the two crystals can be essentially accounted for by the fact that only one crystal, crystal 1, shows sectoral differences in (Na+K).

Table 3 summarizes the amount of sector-zoning of the two crystals

TABLE 3. SUMMARY OF ENRICHMENT ORDERS

Crystal 1				
(100)≈	(110)≈	(010)	> ($\bar{1}$11) in $CaFe^{3+}AlSiO_6$	by 3.8%
(100)			> ($\bar{1}$11) in $CaAlAlSiO_6$	by 5.1%
	(110)		> ($\bar{1}$11) in $CaAlAlSiO_6$	by 4.6%
		(010)	> ($\bar{1}$11) in $CaAlAlSiO_6$	by 2.8%
(100)			> ($\bar{1}$11) in $NaTiAlSiO_6$	by 1.0%
	(110)		> ($\bar{1}$11) in $NaTiAlSiO_6$	by 0.7%
		(010)	> ($\bar{1}$11) in $NaTiAlSiO_6$	by 0.2%
(100)			> ($\bar{1}$11) in $CaTiAl_2O_6$	by 0.9%
	(110)		> ($\bar{1}$11) in $CaTiAl_2O_6$	by 1.3%
		(010)	> ($\bar{1}$11) in $CaTiAl_2O_6$	by 0.7%
Crystal 2				
(100)≈	(110)≈	(010)	> ($\bar{1}$11) in $CaFe^{3+}AlSiO_6$	by 2.9%
(100)			> ($\bar{1}$11) in $CaAlAlSiO_6$	by 2.4%
	(110)		> ($\bar{1}$11) in $CaAlAlSiO_6$	by 1.0%
		(010)	> ($\bar{1}$11) in $CaAlAlSiO_6$	by 2.2%
(100)			> ($\bar{1}$11) in $CaTiAl_2O_6$	by 1.2%
	(110)		> ($\bar{1}$11) in $CaTiAl_2O_6$	by 0.9%
		(010)	> ($\bar{1}$11) in $CaTiAl_2O_6$	by 0.5%

for the several components. In general, the (100) sector is most enriched in all components involving non-divalent cations in the $M1$ and $M2$ positions. For the crystal showing the largest degree of sector-zoning (crystal 1), the (100) sector is enriched relative to the ($\bar{1}11$) sector by about 5 percent $CaAl_2SiO_6$, 4 percent $CaFe^{+3}AlSiO_6$, 1 percent $NaTiAlSiO_6$, and 1 percent $CaTiAl_2O_6$. These differences are balanced by about an 11 percent enrichment of $CaMgSi_2O_6$ in the ($\bar{1}11$) sector.

Discussion

Mechanism of Sector-zoning in Clinopyroxenes. The data presented in this paper suggest that the mechanism of sector-zoning proposed by Hollister (1970) for staurolite needs to be modified if it is to be useful for interpreting sector-zoning in clinopyroxenes. In the staurolite model, it was suggested that rate of growth relative to the diffusion rate perpendicular to the growth surfaces is the factor controlling the presence and magnitude of the sector-zoning. It was further suggested that the composition of the crystallographically different growth surfaces was determined by exchange at the surface, and if the two sites involved in a coupled substitution were exposed simultaneously on a crystal face then the sector behind that face would be enriched in the components involved in the coupled substitution.

For the clinopyroxene, this mechanism does not work in the same manner as for staurolite. On the (010) crystal face (Fig. 8), for example, the $M1$ and T sites are exposed simultaneously, sharing oxygen atoms; and on the (100) face either the M or the T sites are exposed (Fig. 8). Thus, according to the staurolite model, the (010) sector should be enriched in the components $CaAl_2SiO_6$, $CaTiAl_2O_6$, and $CaFe^{+3}AlSiO_6$, relative to the (100) sector. This is the reverse of what is observed (Table 3).

The mechanism proposed for sector-zoning of staurolite could apply to the surfaces of dislocation steps (growth steps), however, because the surface atomic configuration on the (010) face occurs on one surface of a dislocation step associated with growth of the (100) face (Fig. 8), and conversely. Thus, if the chemistry of a sector is determined by the atomic arrangement on a surface of a dislocation step in clinopyroxenes, the staurolite model can be adapted to clinopyroxene. In fact, in discussing possible models to explain sector-zoning in staurolite, it was suggested by Hollister (1970, Model IV, p. 747) that the composition acquired at the surface of a dislocation step could be preserved if re-equilibration at the crystal face was impeded; in the case of staurolite, graphite on the surface was suggested to act as a possible barrier to surface re-equilibration. The importance of the atomic arrangement on the

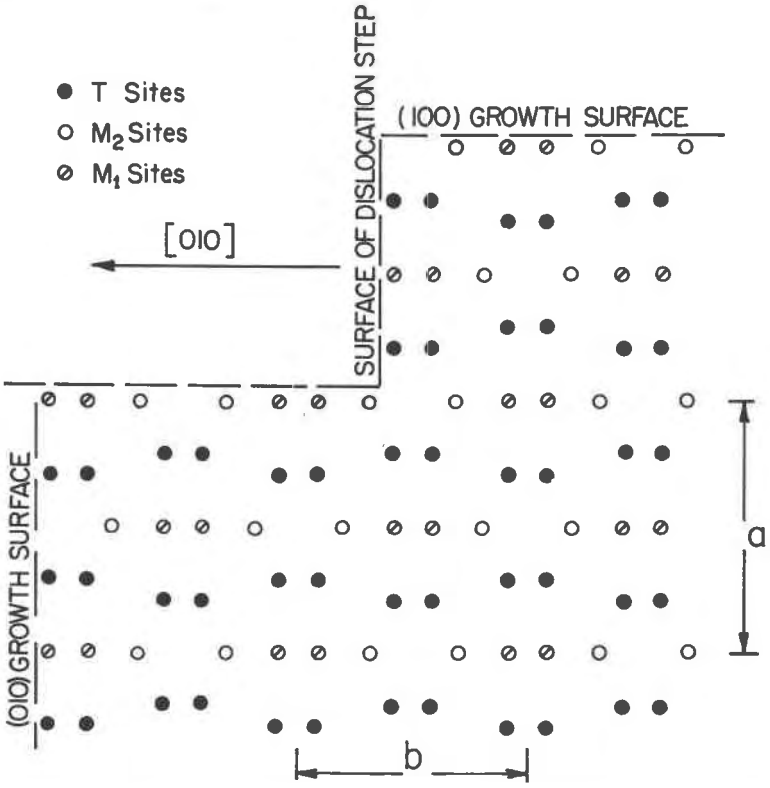

FIG. 8. Sketch showing positions of cations of diopside, as viewed projected on (001). (After Warren and Bragg, 1928.) Illustrated are possible projected cation positions at the (100) and (010) crystal faces and one possible projected cation arrangement at the surface of a dislocation step parallel to (010).

surfaces of growth steps in determining the composition of a sector has been pointed out elegantly by Poty (1969, p. 57) in a discussion of the mechanism of sector-zoning in quartz.

It would appear that Model IV, which was not appropriate to the interpretation of sector-zoning in staurolite, should be re-examined as a possible model to understand sector-zoning in clinopyroxenes. The surface of a dislocation step (Fig. 8), associated with growth of the (100) sector, is certainly favorable for the acquisition of those elements that would be involved in a coupled substitution, and under conditions of rapid crystal growth diffusion perpendicular to the (100) face would effectively be impeded when the next surface layer was added. The com-

position acquired at the surface of the dislocation step would then be preserved by growth because clinopyroxene in volcanic rocks is probably a refractory mineral as defined by Hollister (1969).

Besides the atomic arrangements on surfaces of dislocation steps or on crystal faces, the size of an individual block of material which is added at one time to a crystal may be another important factor which will affect the development of compositional sector-zoning. If the block of material is large (for example, a group of polymerized chains in a melt), the initial composition acquired at a dislocation step would be dependent on the average composition of the block of material as it existed in the melt. If this were the case, the initial composition on each sector would be the same and subsequent exchange of material across the surface of the growth step would be required to produce sectoral differences in composition.

Thus, at least four factors are envisaged to affect the presence and magnitude of sector-zoning: (1) rate of addition of material to a crystal, (2) size and composition of blocks of material added to the crystal at any one time, (3) rate of equilibration of the new block of material with the matrix at the surfaces of dislocation steps, and (4) rate of re-equilibration of surface layers with the matrix by exchange of ions perpendicular to the crystal faces. The following four cases illustrate how these four factors can interrelate to lead to the development of compositional sector-zoning.

A very rapidly grown crystal (Case A) would have its chemistry dependent only on that which was acquired at the growth step by addition of ionic complexes as blocks (polymerized chains?) of material. In this case, the chemistry of all sectors would be the same, if the matrix were homogeneous. The bulk chemistry of the crystal would be most dependent on the initial chemistry of the matrix (solid or liquid) and perhaps not be dependent at all on equilibrium factors. A crystal which grew more slowly (Case B, equals Model IV for staurolite), but still relatively fast compared to the next two cases, would have sufficient time for surface equilibrium to be achieved between the surface of the growth step and the matrix, but would not have sufficient time for equilibrium to be achieved between the crystal surface itself and the matrix. Still slower growth (Case C, equals Model III for staurolite) would allow equilibrium to be achieved between the growth surface and the matrix. The re-equilibration between the growth surface and the matrix would change the chemistry previously acquired by equilibration between the surface of the dislocation step and the matrix because the two dimensional atomic configurations would be different in the two cases. Finally, a very

slowly grown crystal (Case D) would be expected to achieve complete equilibrium between the matrix and the three dimensional regions of the crystal, identical in all parts of the crystal.

Case A would give the same chemistry on all faces, regardless of surface atomic configurations; growth faces may, in fact, not exist in this case. Only continuous radial zoning would be observed and that only if the composition of the matrix changed during crystal growth. For Cases B and C, the crystal would be sector-zoned, but the enrichment of elements in one sector relative to the other would be reversed because the two dimensional atomic arrangements on the average surface of the growth steps of one growth face are similar to those on one or (at a different stage of growth) more of the other growth faces. For Case D, the crystal would not show sectoral differences in composition, as in Case A, but the composition of the crystal would be dependent on thermodynamic equilibrium conditions, including the composition of the matrix.

The two best-documented cases for major differences in elements between sectors, staurolite and clinopyroxene, are considered examples of Cases C and B, respectively. The staurolite, grown in a solid matrix under metamorphic conditions, probably grew at a slower rate than clinopyroxenes in rapidly cooled melts, either terrestrial or lunar. Saurolite (Hollister, 1970) was shown to be sector-zoned by a mechanism involving exchange across the growth surface. Given a decrease in the linear rate of growth of a crystal, each successive growth surface is exposed to the matrix for a longer and longer period of time as the crystal grows bigger. This implies that the degree of sector-zoning, the magnitude of differences in composition between sectors, will decrease with growth. It was shown (Hollister, 1970) that for staurolite this is observed.

For Case B, on the other hand, as it is approached from Case A, the reverse result might be produced. Here a very rapidly grown crystal will not be sector-zoned (Case A) but as its linear rate of growth slows as it becomes bigger it would be expected to develop sector-zoning; and as its linear rate of growth slows even more with increasing growth, allowing more time for exchange to take place across the surface of growth steps, the magnitude of sector-zoning might actually increase with growth. Finally, as the rate of crystal growth slowed to zero, Case C might become dominant and the relative order of enrichment might even reverse itself at the very edge of the crystal. The data on the sector-zoning of the clinopyroxenes from Italy are consistent with Case B being approached from Case A: the magnitude of sector-zoning (Table 3) is less in the section cut closer to the center of the crystal (Figs. 2b and 3b) than for the section cut further from the center of a different crystal (Figs. 2a and 3a).

This discussion must be regarded as preliminary because it is based on a comparison of sector-zoning on two quite different minerals which have grown in two very different environments. The staurolite grew in a solid matrix and the clinopyroxene in a melt. It is probable that the nature of the material added to the crystal at any one instance is critical in determining the type of sector-zoning. In the solid matrix the blocks of material added at one time to the crystal may be small ionic complexes, perhaps involving only one cation, whereas in a silicate melt several large polymerized chains may be added at one time; for a crystal growing from a vapor or aqueous phase, other mechanisms for addition of materia- may be envisaged. More documented examples of sector-zoning are required before a uniform theory of compositional sector-zoning can be developed and before valid geologic conclusions can be made based on sector-zoning effects.

Sector Zoning in $CaAl_2SiO_6$. The data presented in this paper (Fig. 4 and Table 3) clearly show that clinopyroxenes can be sector-zoned in the component $CaAl_2SiO_6$, a component whose concentration is believed to be sensitive to pressure. The interpretation of sector-zoning (Hollister, 1970) implies, of course, that the different compositions of sectors are preserved from differences in composition acquired at the surface under identical conditions of pressure, temperature, and composition of matrix. Because sector-zoning can result from rapid growth, with variation of sectoral differences produced by differing growth rates, it follows that the bulk composition of a sector, or of the whole crystal, may be dependent on the rate of growth. In fact, the dependence of the composition of a crystal on the rate of growth of a crystal has been known for some time (see discussion in Hollister, 1970, p. 745). These observations therefore suggest that caution should be exercised in the application of the presence of $CaAl_2SiO_6$ in clinopyroxenes to the interpretation that they grew at significant pressure. This caution should especially be applied to the lunar clinopyroxenes where there is substantial evidence for rapid crystallization; however, it has been proposed (Bence, *et al.*, 1970b) that the presence of $CaAl_2SiO_6$ in the clinopyroxene phenocrysts in some Apollo 12 samples may suggest that the magmas at the Apollo 12 landing site were generated in the lunar interior.

Our suggestion that the presence of $CaAl_2SiO_6$ in a crystal is dependent on growth-rate phenomena should not be taken to imply that the presence of this component should be discounted as a pressure indicator. The evidence is strong (Kushiro, 1962; 1965) that in the presence of anorthite, under equilibrium conditions, the amount of $CaAl_2SiO_6$ in clinopyroxenes is dependent on pressure. In the present study, the clinopyroxenes did

not crystallize with anorthite. On the other hand, the average coordination of aluminum in the melt may be pressure dependent and, if material is added to the crystal as ionic complexes, possibly as polymers, the aluminum coordination of the initial material added to the crystal may reflect the state of aluminum coordination in the melt. The fact that the aluminum content is higher in all sectors close to the centers of the crystals from the Narce area (Fig. 3) may reflect initial nucleation of the crystals at high pressure in a melt of high average aluminum coordination because the initial linear rate of growth may have been sufficiently high that Case A would apply.

Acknowledgments

The samples used in this study were collected by one of us (A.J.G.) during the course of a field study for a B.A. thesis at Princeton under the guidance of Professor Sheldon Judson. Financial support for the field work was provided by the John Boyd Memorial Fund of Princeton University and by American Overseas Petroleum, Ltd.

C. Kulick, T. Loomis, and R. Warren assisted in the collection and reduction of the microprobe data. We thank R. Hargraves and D. Waldbaum for comments on the manuscript. Discussions with D. Lindsley (SUNY-Stony Brook) and B. Poty (Université de Nancy) contributed to the content of this paper. Financial assistance for the laboratory work was provided by NASA contract NAS 9-7897 and by NSF grant GA 20236.

References

Albee, A. L., and A. A. Chodos (1970) Microprobe investigations on Apollo 11 samples. *Geochim. Cosmochim. Acta, Proceedings of the Apollo* 11 *Lunar Science Conference* **1,** 135–158.

———, and L. Ray (1970) Correction factors for electron probe microanalysis of silicates, oxides, carbonates, phosphates, and sulphates. *Anal. Chem.* (in press).

Bence, A. E., and A. L. Albee (1968) Empirical correction factors for the electron microanalysis of silicates and oxides. *J. Geol.* **76,** 382–403.

———, K. Cameron, and J. J. Papike (1970a) Sector zoning in calcic clinopyroxenes. *Trans. Amer. Geophys. Union* **51,** 435.

———, J. J. Papike, and C. T. Prewitt (1970b) Apollo 12 clinopyroxenes: Chemical trends. *Earth Planet. Sci. Lett.* **8,** 393–399.

Binns, R. A., M. B. Duggan, and J. F. G. Wilkinson (1970) High pressure megacrysts in alkaline lavas from northeastern New South Wales. *Amer. J. Sci.* **269,** 132–168.

Clark, S. P., Jr., J. F. Schairer, and J. de Neufville (1962) Phase relations in the system $CaMgSi_2O_6$-$CaAl_2SiO_6$-SiO_2 at low and high pressure. *Carnegie Inst. Wash. Year Book* **61,** 59–58.

Gancarz, A. J. (1970) *Geology of the Volcanic Rocks of the Treia River Basin, Italy.* B.A. thesis, Princeton University.

Hargraves, R. B., L. S. Hollister, and G. Otalora (1970) Compositional zoning and its significance in pyroxenes from three coarse-grained lunar samples. *Science* **167,** 631–633.

Hollister, L. S. (1969) Contact metamorphism in the Kwoiek area of British Columbia: an end member of the metamorphic process. *Geol. Soc. Amer. Bull.* **80,** 2465–2494.

———, (1970) Origin, mechanism, and consequences of compositional sector-zoning in staurolite. *Amer. Mineral.* **55,** 742–766.

———, AND R. B. HARGRAVES (1970) Compositional zoning and its significance in pyroxenes from two coarse grained Apollo 11 samples. *Geochim. Cosmochim. Acta, Suppl.* 1, **1,** 541–550.

KUNO, H. (1964) Aluminian augite and bronzite in alkali olivine basalt from Taka-simor, north Kyushu, Japan. *In Advancing Frontiers in Geology and Geophysics*. Hyderabad, Osmania Univ. Press, 205–220.

KUSHIRO, I. (1962) Clinopyroxene solid solutions, pt. 1, The $CaAl_2SiO_6$ component. *Jap J. Geol. Geog.* **33,** 213–220.

———, (1965) Clinopyroxene solid solutions at high pressures. *Carnegie Inst. Wash. Year Year Book* **64,** 112–117.

MARINELLI, G., AND M. MITTEMPERGHER (1966) On the genesis of some magmas of typical Mediterranean suite. *Bull. Volcan.* **29,** 113–140.

MATTIAS, P. (1968) *Carta Geologica Regione Vulcanica dei Monti Sabatine e Cimini*. Servizio Geologica d'Italia, Roma.

POTY, B. (1969) La croissance des cristaux de quartz dans les filons sur l'exemple du filon de La Gardette (Bourg d'Oisans) et des filons du massif du Mont-Blanc. Sci. Terre, Mem. 17, 162 pp.

———, (1966) La croissance du quartz lamellaire sur l'exemple des cristaux de la Gardette (Osére, France). *In Proceedings International Mineralogical Association, 5th Meeting Cambridge, 1966*. Mineralogical Society of London, p. 54–62.

STRONG, D. F. (1969) Formation of the hour-glass structure in augite. *Mineral. Mag.* **37,** 472–479.

WARREN, B. E., AND W. L. BRAGG (1928) The structure of diopside CaMg $(SiO_3)_2$. *Z. Kristallogr.* **69,** 168.

WASHINGTON, H. S., AND H. E. MERWIN (1921) Notes on augite from Vesuvius and Etna. *Amer. J. Sci.* **50,** 20–30.

Manuscript received, October 26, 1970; accepted for publication, November 17, 1970.